Adv Polym Sci (2005) 177: 151–179
DOI 10.1007/b101377

Poly(arylene ethynylene)s in Chemosensing and Biosensing

Juan Zheng · Timothy M. Swager (✉)

Department of Chemistry, Massachusetts Institute of Technology, 77 Massachusetts, Avenue, Cambridge, MA, 02139 USA
tswager@mit.edu

Abstract Poly(arylene ethynylene)s (PArEs) have been used in recent years as effective transducers for a variety of sensing purposes ranging from organic molecules such as methyl viologen and TNT to biological analytes. Their superior sensitivity to minor perturbations is fundamentally governed by the energy transport properties resulting from the extended conjugation of the polymer backbone. An understanding of the underlying principles of energy transport allows the design of sensors with greater sensitivity and specificity. Pioneering work with methyl viologen as an electron-transfer quencher demonstrated that connecting receptors in series amplifies the sensing response compared to that of individual receptors. Since then, factors such as the electronic and structural nature of the polymers and their assembly architecture have proven to be important in improving sensory response. In this review, we present an overview of works to date by various groups in the field of PArE chemosensors and biosensors.

Keywords Poly(arylene ethynylene) · Chemosensor · Biosensor · Fluorescence · Energy transfer

Abbreviations and Symbols

ALF	Anthrax lethal factor
DNT	2,4-Dinitrotoluene
FRET	Fluorescence resonance energy transfer
MBL-PPV	Poly[lithium 5-methoxy-2-(4-sulfobutoxy)-1,4-phenylene vinylene]
MPS-PPV	5-Methoxy-5-propyloxy sulfonate phenylene vinylene
MV^{2+}	Methyl viologen
PArE	Poly(arylene ethynylene)
PNA	Peptide nucleic acid

PPE	Poly(phenylene ethynylene)
PPV	Poly(phenylene vinylene)
TIPS	Triisopropylsilyl
TNT	2,4,6-Trinitrotoluene

1 Introduction

An ideal sensor recognizes analytes in a sensitive, selective, and reversible manner. This recognition is in turn reported as a clear response. In recent years, conducting polymers have emerged as practical and viable transducers for translating analyte–receptor and nonspecific interactions into observable signals. Transduction schemes include electronic sensors using conductometric and potentiometric methods and optical sensors based on colorimetric and fluorescence methods [1].

Poly(arylene ethynylene)s (PArEs) are wide-gap semiconductors. They are typically insulating in their native neutral state but can be made conductive by either oxidizing or reducing the polymer's π-electron system (doping) [2, 3]. Their semiconductive nature has generated interest in developing electroluminescent polymers for device applications [4–6]. However, it is their photophysical characteristics that make PArEs good candidates for use as transducers, and they are now one of the most important classes of conducting polymers for sensing purposes. In this review, we will focus on colorimetric and fluorescence detection methods using PArE sensors. Some ingenious chemo- and biosensors that employ conducting polymers other than PArEs will also be highlighted. There are currently many research groups in the field of conjugated polymer sensors and interested readers are directed to previous reviews [1, 7 and references therein].

2 PArEs for Signal Amplification

In analogy to traditional semiconductors, the extended electronic structures of PArEs can be visualized using energy bands composed of a valence band and a conduction band. Excited states consisting of electron–hole pairs, also referred to as excitons, can be generated upon photoexcitation and these travel through the polymer energy bands by Förster or Dexter mechanisms. One may consider the PArE as a molecular wire for exciton transport. Recombination of the electron–hole pairs can occur via radiative and nonradiative pathways, and the emissive properties of conjugated polymers are dominated by energy migration to and exciton recombination at the local minima of their band structures. Therefore, perturbations to the PArE will be reflected in

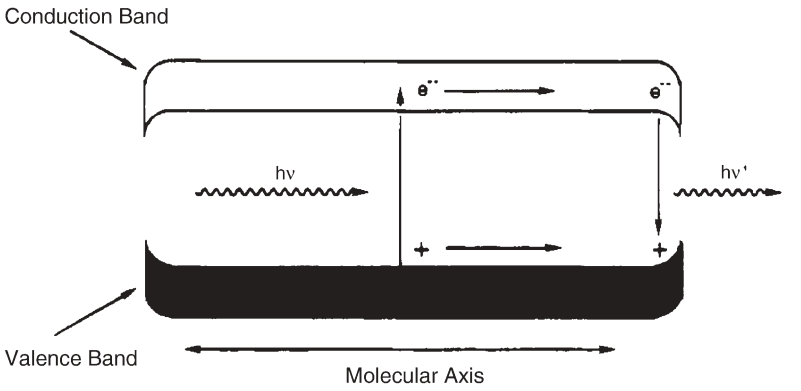

Fig. 1 Energy migration in a semiconductive molecular wire with a decrease in bandgap at the terminus. (Reprinted with permission from Ref. [8]. Copyright 1995 American Chemical Society)

its collective property. This has important implications for sensing applications.

The sensitivity of poly(phenylene ethynylene)s (PPEs) to perturbations in their band structure is illustrated by end-capping PPEs with anthracene units (**1**). The polymers act as antennae for harvesting optical energy and this is transferred to the anthracene units due to an induced localized narrowing of the bandgap (Fig. 1). Radiative recombination of the electron–hole pair results in greater than 95% of the emission occurring at the states localized at the anthracene end groups [8]. The presence of anthracene is effectively amplified.

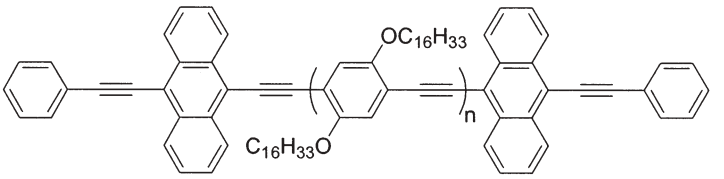

1

This amplification phenomenon can be applied to sensor design and was first demonstrated by our group in 1995 [9, 10]. In these studies, the sensing ability for a methyl viologen salt (MV^{2+} or *N*,*N*′-dimethyl-4,4′-bipyridinium bis(hexafluorophosphate)) is measured for a fluorescent single receptor molecule **2** and a PPE **3** where many receptors are "wired in series". In this sensing scheme, excitons were generated by photoexcitation of the polymer. When they encounter a cyclophane-bound MV^{2+}, a highly efficient electron-transfer reaction occurs to the analyte and the initially fluorescent polymer is returned to the ground state without the emission of a photon (Fig. 2). A 67-fold increase

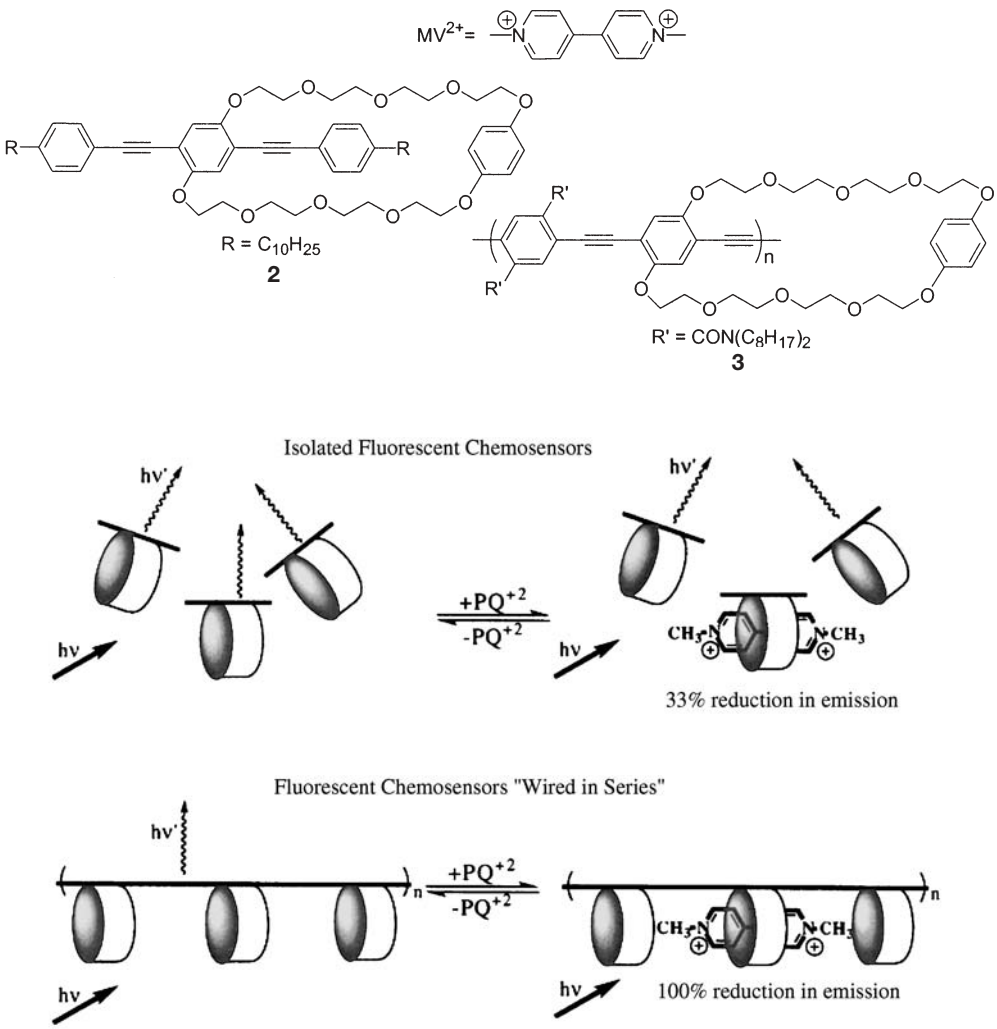

Fig. 2 Conceptual illustration of signal amplification by wiring receptors in series. (Reprinted with permission from Ref. [10]. Copyright 1995 American Chemical Society)

in quenching enhancement was obtained by comparing the Stern–Volmer quenching constants (K_{SV}) for **3** and **2**, corresponding to an average of 134 phenylene units sampled by the excitons. The quenching efficiency of MV^{2+} increased steadily with increasing polymer molecular weight, reaching a maximum at 65,000 and plateaued thereafter. The molecular weight dependence of quenching indicated that the diffusion length of the exciton is less than the length of the polymer. Polymers **4** and **5** were also synthesized and lower enhancement of quenching was observed in both cases in comparison to **3.** The *meta*-substituted comonomer in **4** resulted in a polymer with decreased delo-

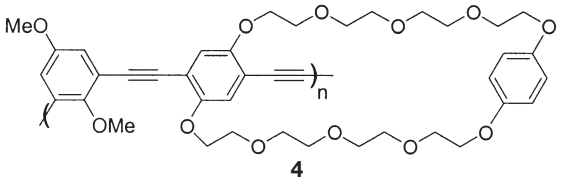

4

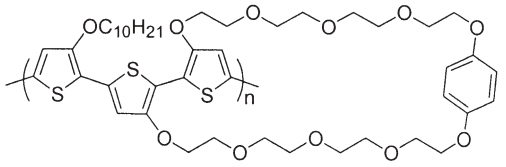

5

calization and decreased energy migration efficiency, culminating in diminished quenching. However, the greater delocalization of polythiophene **5** did not guarantee a more efficient energy migration; a decrease in its fluorescence efficiency was instead the determining factor.

The apparent binding constant K_{SV} obtained by Stern–Volmer quenching studies is the product of the number of receptors visited by the exciton and the binding constant of MV^{2+} to the cyclophane receptor. For this reason polymer **3** and its monoreceptor model **2** were designed so that the binding constant for methyl viologen to the receptor was known for both systems. This allowed the calculation of the true amplification factor of 67.

Whitten et al. have since applied the energy transport properties of conjugated polymers to amplified quenching studies [11]. In their work, the anionic conjugated polymer **6**, 5-methoxy-5-propyloxysulfonate phenylene vinylene (MPS-PPV), was quenched using the cationic methyl viologen. The Stern–Volmer quenching constant was reported to be ~10^7 M^{-1} and more than a million-fold amplification relative to the neutral small molecule model **7** was suggested. However, these numbers are misleading, firstly because the K_{SV} is a combination of the amplification factor and the binding constant of MV^{2+} with the anionic PPV, and secondly because the small molecule model is not a reasonable analog of the receptor–analyte recognition and so an accurate binding constant cannot be obtained. Since the MV^{2+} is reported to quench at a level of 95% when the viologen concentration is 1/100 that of the repeat unit, the amplification is likely overestimated by as much as 10^4–10^5.

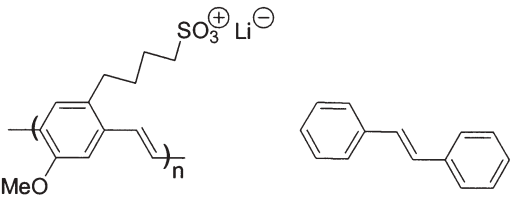

6 **7**

Anionic PPEs with higher quantum yields than MPS-PPV that are also quenched by MV^{2+} have been synthesized by Schanze et al. In methanol, sulfonated PPE **8** and its small molecule analog **9** expressed K_{SV} values of 1.4×10^7 M^{-1} and 2.2×10^4 M^{-1}, respectively. In water, the K_{SV} values were 2.7×10^7 M^{-1} and 7.0×10^3 M^{-1} for the two species [12]. The polymer was aggregated in water but not in methanol and greater amplification was seen in the former solvent. Since aggregation of the polymer is induced by the addition of only a few quenchers per chain, this may contribute to the increased response due to self-quenching. Phosphonated PPEs such as **10** have also been prepared by the same group [13]. In this case, the amplification was ~100-fold compared to a small molecule model **11** with the MV^{2+} quencher. Interestingly, similar quenching amplification factors were observed with cationic dyes such as ethydium bromide and rhodamine 6G, which shunt the polymer emission via a singlet–singlet Förster energy-transfer mechanism. As MV^{2+} precludes a Förster mechanism for quenching the polymer, such long-range transfer from a polymer to a dye acceptor may not be necessary.

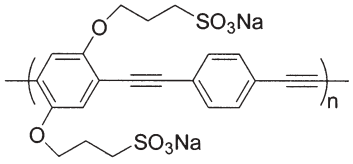

8

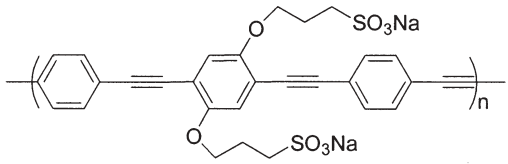

9

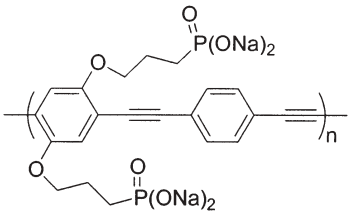

10

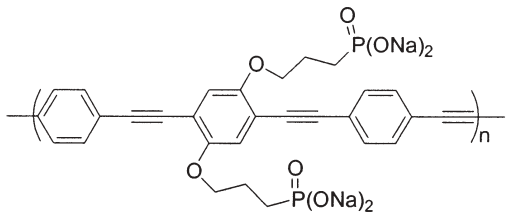

11

The 67-fold amplification obtained for polymer **3** is restricted by an inherent limitation of the "wired in series" design. As the exciton travels in a one-dimensional random walk process down the polymer chain, it has equal opportunity to visit a preceding or an ensuing receptor. This represents 134^2 random stepwise movements for 134 phenylene ethynylene units, and so much of the receptor sampling by the exciton is redundant. Increasing the efficiency of receptor sampling requires maximization of the number of different receptors that an exciton can visit throughout its lifetime. To achieve this end we extended the polymer sensor into two dimensions by use of a thin film and thereby increased the sensitivity.

PPEs often π-stack and form excimers in the solid state [14–17]. To circumvent this problem we designed PPE films that incorporate rigid three-dimen-

sional pentiptycene scaffolds in the polymer backbone [18, 19]. These polymers form porous films and discriminately bind to various analytes of suitable size and electronic properties. Strongly electron-deficient analytes such as 2,4,6-trinitrotoluene (TNT) and 2,4-dinitrotoluene (DNT) cause fluorescence quenching by an electron-transfer mechanism. Films of polymer **12** were quenched by 50% within 30 s of exposure to TNT and by 75% within 60 s, despite the low equilibrium vapor pressure of 7 ppb for the analyte (Fig. 3 and Fig. 4).

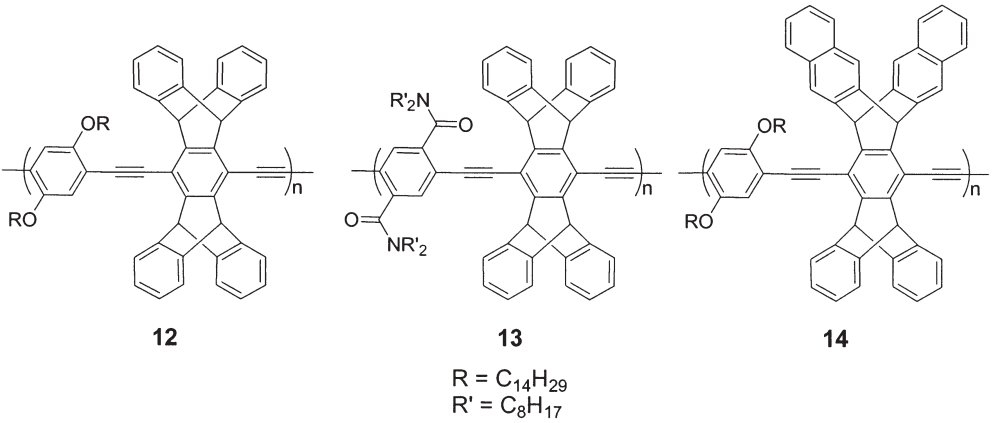

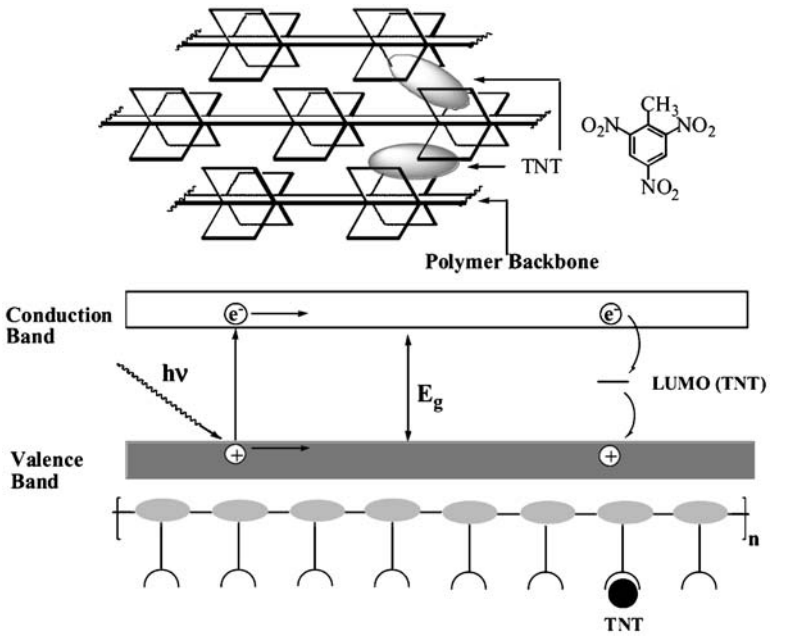

Fig. 3 *Top*: Schematic representation of porous polymer films allowing for analyte docking. *Bottom*: Band diagram depicting quenching resulting from electron transfer from PPE to TNT.

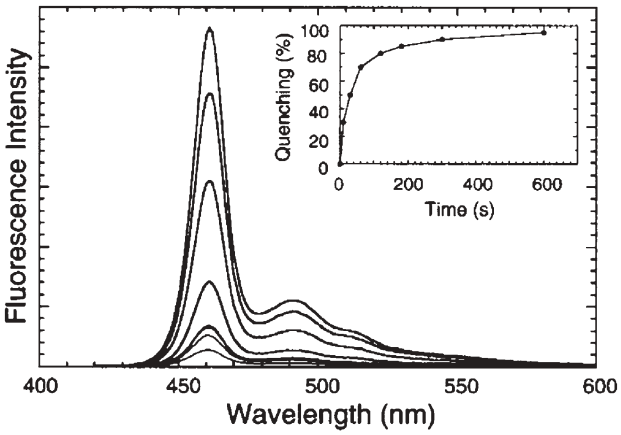

Fig. 4 Time-dependent fluorescence intensity of **12** upon exposure to TNT vapor at 0, 10, 30, 60, 120, 180, 300, and 600 s (*top to bottom*), and fluorescence quenching (%) as a function of time (*inset*). (Reprinted with permission from Ref. [18]. Copyright 1998 American Chemical Society)

Films of varying thicknesses were investigated. In thick films of **12** at 200 Å, analytes such as duroquinone that had fewer electrostatic interactions with the polymers diffused to greater depths and so better cumulative quenching was observed. In the case of electron-deficient nitro compounds, the stronger electrostatic interactions limited their diffusion in thicker films, resulting in a smaller quenching response. However, in thin films of 25 Å, nitroaromatic compounds displayed superior quenching effects to those of quinones due to stronger film interactions, despite their lower vapor pressures and thermodynamically less favorable electron-transfer reactions.

The polymer composition was varied in order to probe the effects of polymer electronic and steric properties on analyte binding (structures **13** and **14**). As expected, the electron-deficient polymer **13** was less sensitive to oxidative quenchers. Steric factors were also important, as larger molecules had slower rates of diffusion through film cavities that were obstructed by the nonplanar structure and the double alkyl chains of the amide groups in **13**. Interpolymer interactions between the naphthalenoid pentiptycenes and adjacent polymer backbones in **14** also resulted in smaller cavity sizes and slower analyte diffusion. A good balance of electrostatic interactions and film porosity is therefore crucial to the design of a sensitive optical sensor for TNT. Detectors based on this technology are currently being manufactured by Nomadics Inc. and have been shown to be effective in detecting landmines in the field [20].

As greater sensitivity was realized in 2D compared to 1D, to further maximize the sensitivity of the polymer we investigated energy migration in three dimensions. The Langmuir–Blodgett technique was used to construct layers of aligned PPE in order to facilitate dipolar Förster-type processes for efficient intermolecular energy transfer from the PPE to surface acridine orange ac-

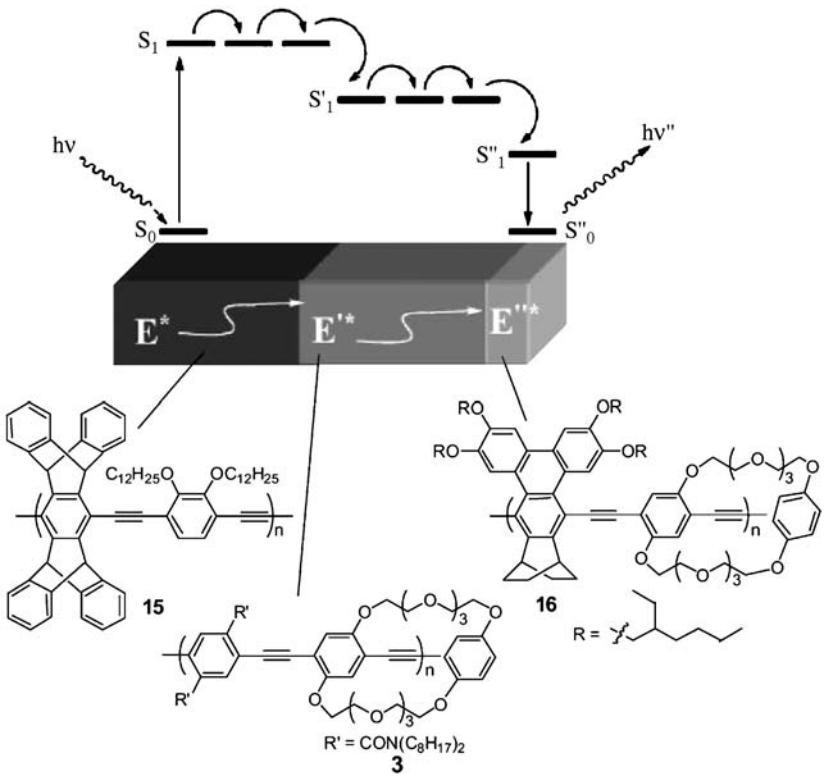

Fig. 5 Energy transfer from polymers **15** to **3** to **16**. The films have decreasing bandgaps moving from the *bottom* to the *top*. Polymer **15** (abs./em. max. 390/424 nm) overlaps with **3** (abs./em. max. 430/465 nm) overlaps with **16** (abs./em. max. 495/514 nm). (Reprinted with permission from Ref. [22]. Copyright 2001 American Chemical Society)

ceptors [21]. Increasing the number of polymer layers steadily enhanced the acridine orange emission with the energy transfer peaking at 16 layers. This may at first glance seem counterintuitive since the relative amount of acridine orange acceptors to polymer donor decreases as the polymer thickness increases. However, in analogy to the amplification observed for the two-dimensional process discussed earlier, the energy trapping efficiency is maximized in 3D as the exciton does not retrace its steps. Enhanced acridine orange emission is therefore observed with thicker films. These insights have been applied to directed energy transfer with PPEs by layering polymer films with decreasing bandgaps on top of one another (Fig. 5) [22]. Energy is preferentially transferred to the surface of the thin film, where the bandgap is the smallest. This ability to control the exciton pathway has important implications for the design of chemosensors.

Polymers with extended lifetimes can have excitons with higher diffusion lengths and hence a greater probability of encountering a receptor-bound an-

alyte. Polymers **17** and **18** were synthesized to this effect. Incorporation of triphenylenes into **17** enhanced the lifetimes of the polymer by about 30% compared to those of the PPE analog. Dexter energy transfer was determined to be the dominant intramolecular energy transport process in these poly(triphenylene ethynylene) materials [23]. PArE **18** and related polymers based on dibenzo[*g*,*p*]chrysene also display long excited lifetimes in the range of 1.4–2.6 ns. These polymers are promising materials for sensing applications.

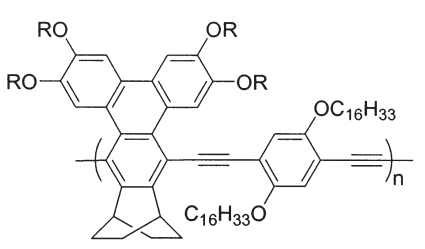

17

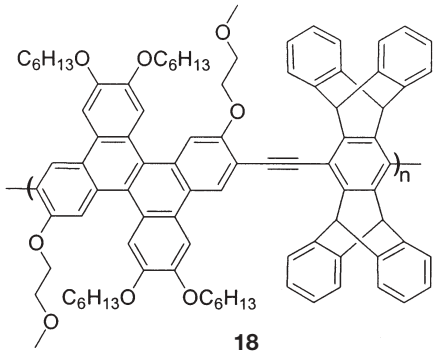

18

3 PArEs with Specific Receptors

The excellent amplifying abilities of PArEs are advantageous to sensor design. However, adequate and specific receptors are also of crucial importance. Conjugated polymers with custom receptors, for use in the detection of heavy-metal contaminants, were presented by Wasielewski et al. in 1997. In this study, the polymer incorporated 2,2′-bipyridyl ligands in the backbone, which could coordinate to a wide variety of metal ions. Metal sensing is realized by inducing changes in the degree of conjugation in poly(phenylene vinylene)s, thereby influencing their bandgap and affecting their absorption and fluorescence spectra [24].

In its *transoid* form, a 20° dihedral angle exists between the two pyridine rings in 2, 2′-bipyridine and as a result, polymers **19** and **20** are not fully conjugated. When chelated to a metal ion, the coordination between the metal ion

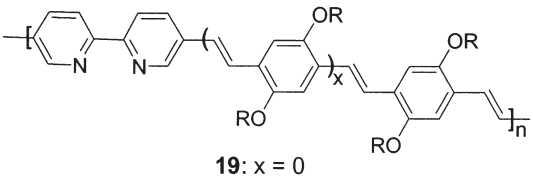

19: x = 0
20: x = 2
R = $C_{10}H_{21}$

and the bipyridine would forcefully planarize the initially twisted conformation, thereby increasing the conjugation. Metals such as Zn^{2+}, Cd^{2+}, Hg^{2+}, Ag^{+}, Al^{3+}, and lanthanide ions caused a significant redshift in the polymers' absorption and fluorescence with minimal fluorescence quenching. This redshift can be explained by a conjugation enhancement due to metal binding and to a lesser extent, due to the electron density variations on the polymer backbone by coordinating to electron-deficient metal ions. Other metal ions such as Pb^{2+}, Fe^{2+}, Fe^{3+}, Cu^{+}, Sb^{3+}, and certain lanthanide ions caused a blueshift in the fluorescence spectra with significant quenching. This was explained by a monodentate binding of metal ion to bipyridyl ligands, which induced a more twisted backbone and hence a decrease in the conjugation of the polymer. Cu^{2+}, Ni^{2+}, Co^{2+}, Mn^{2+}, Sn^{2+}, and Pd^{2+}, on the other hand, quenched the fluorescence quantitatively due to energy- or electron-transfer reactions between the phenylene vinylene segments and the metal complexes. Absorption and fluorescence spectral profiles were dependent on the metal complex and the ions may be removed by treatment with competing ligands such as ammonium and cyanide ions.

In accordance with Wasielewski's report, Huang et al. synthesized three polymers with different linkers between the chromophores (**21**–**23**), including a PArE derivative, to study the effect of polymer backbone extension and rigidity on the sensitivity and selectivity of bipyridyl-based metal sensors [25]. The polymers were very responsive to transition metal ions (typically in the micromolar range, 10^{-6} M) and insensitive to alkali and alkaline earth metals with the exception of Mg^{2+}. Decreasing sensitivity was observed as the polymer was varied from **21** to **23**. For transition metal ions in the 2nd and 3rd groups, the least amount of analyte was required to quench **21**, while **22** and **23** required progressively larger amounts of analyte to effect quenching.

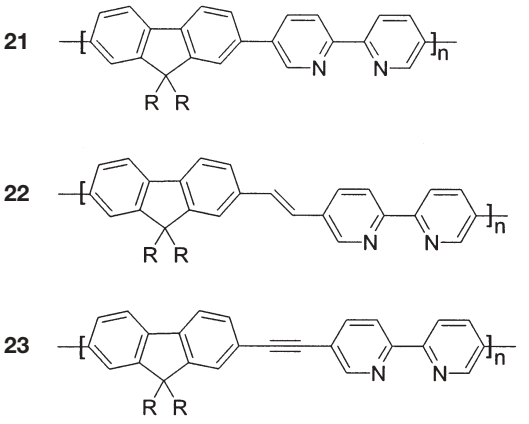

PArEs with pendant bipyridyl or terpyridyl ligands have also been reported [26]. At 3.08×10^{-6} M polymer concentration, a Ni^{2+} concentration of 1.0×10^{-6} M quenched **24** and **25** to 10.9 and 38.2% of their respective initial fluorescence

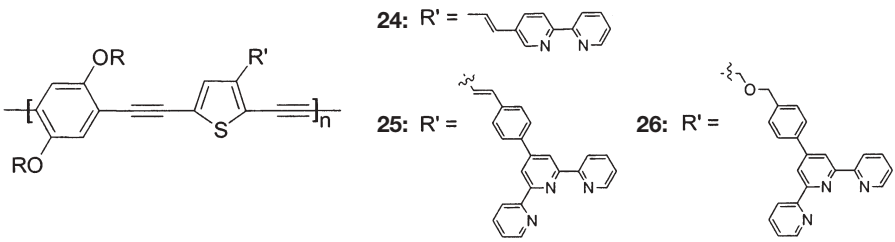

emissions. Polymers with ligands linked via a vinylene linkage were therefore more sensitive than those where the ligands were connected via an ether linkage, highlighting the importance of electronic communication for increased sensitivity. Selectivity toward different transition metals was mediated by the chelating ability of the terpyridine ligand. PArE **24** showed response to Cr^{6+}, Cd^{2+}, Ni^{2+}, and Mn^{2+}, while Na^{+}, Ca^{2+}, Pb^{2+}, and Hg^{2+} did not elicit any sensory response (Fig. 6). Consistent with the tridentate nature of terpyridine, polymers substituted with this ligand were more sensitive than the bidentate bipyridine-substituted PArE **26.**

The same group has synthesized well-defined porphyrin-containing PArEs **27** and **28** [27]. The central metal cation could complex to various solvent ligands. Depending on the electron-donating ability of the solvent ligand, complexation of solvent to metal ion changes the electron density on the porphyrin

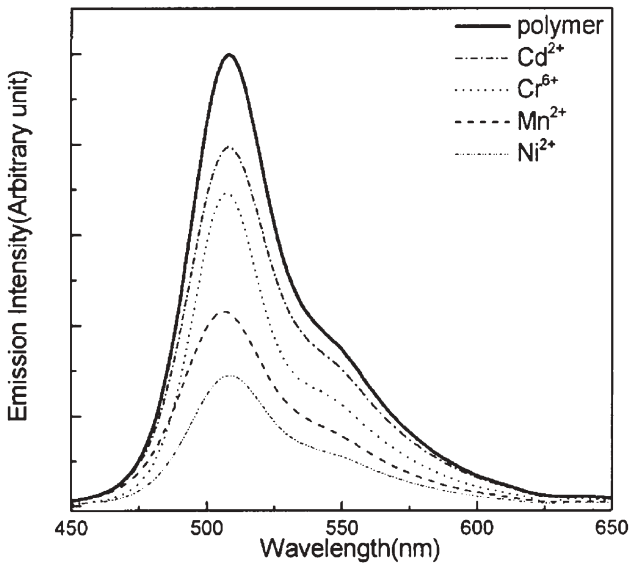

Fig. 6 Emission quenching of polymer **25** by different transition metal ions. The polymer concentrations are held fixed at 3.08×10^{-6} M corresponding to receptor unit. Transition metal ions are 1.54×10^{-6} M. (Reprinted with permission from Ref. [26]. Copyright 2002 American Chemical Society)

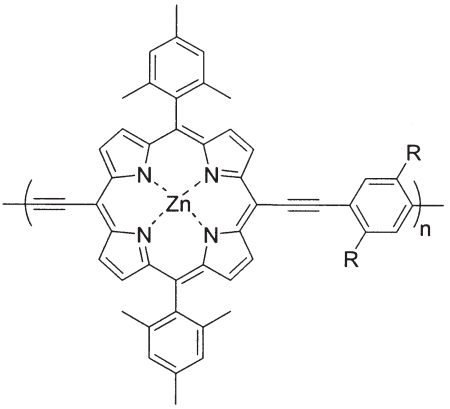

27: R = $O_{15}H_{31}$

28: R = $CON(C_8H_{17})_2$

units. For basic solvents, an increase in electron density leads to a redshift in the absorption and emission bands of the polymers. For instance, on going from chloroform to *n*-butylamine, the emission shifted from 704 to 741 nm. The coordinating ability of the central metal cation and the tunability of the PArE polymer could potentially be used for optical sensors.

Other polymers with coordinating abilities such as quinoline-containing PArEs **29** and **30** have also been synthesized by Bunz et al. [28]. In this case, the polymers were sensitive to metal ions such as Pd^{2+}, La^{3+}, and Ag^{+}.

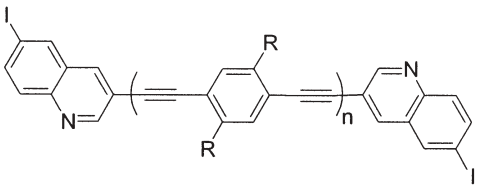

29 R = 2-ethylhexyl

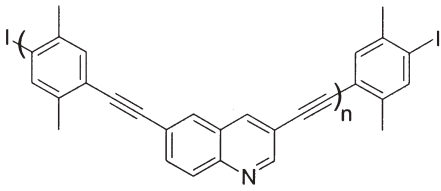

30

While aggregation is usually an undesired characteristic for PArEs, we have seized the accompanying spectral changes of this phenomenon for sensing purposes. This was demonstrated by the detection of potassium ions with use of a 15-crown-5-substituted PPE [29]. K^{+} induces a 2:1 complex with 15-crown-5 while Li^{+} and Na^{+} form 1:1 complexes with the same crown ether. As a consequence, aggregation between polymer chains occurs only with K^{+} and this was observed at a polymer-to-ion ratio of 0.5:1 (Fig. 7). This was manifested by a diminished emission and appearance of a bathochromic band in the absorption spectrum upon addition of K^{+} to a solution of **31**, consistent with spectra obtained by compressing the polymer film at the air–water interface (Fig. 8). No change in the absorbance and emission spectra was observed even at 1,500-fold excess of Na^{+} and Li^{+}. The comonomer's steric and electronic properties were important in facilitating π-stacking interactions between poly-

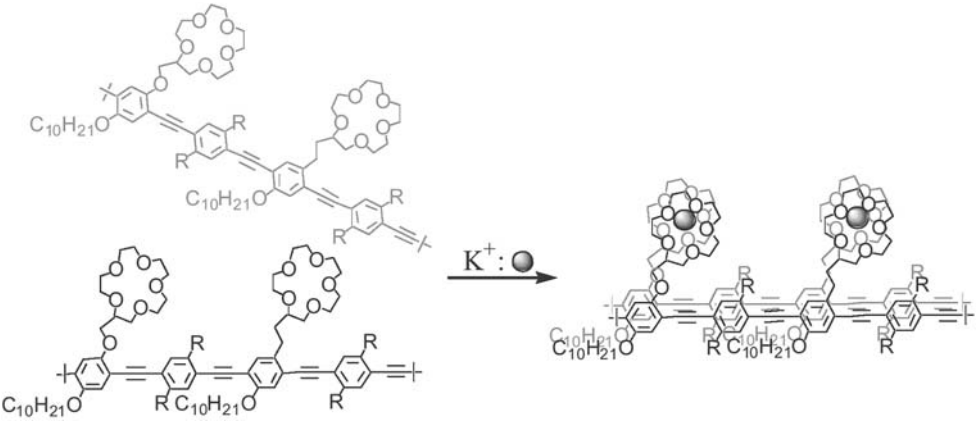

Fig. 7 Schematic representation of K^+ ion-induced aggregation. (Reprinted with permission from Ref. [29]. Copyright 2000 Wiley-VCH Verlag GmbH)

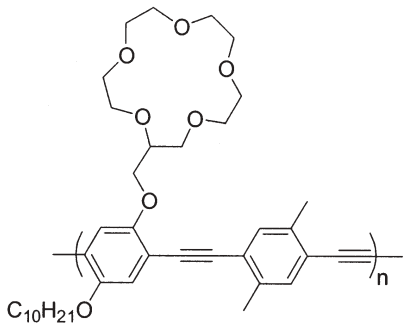

31

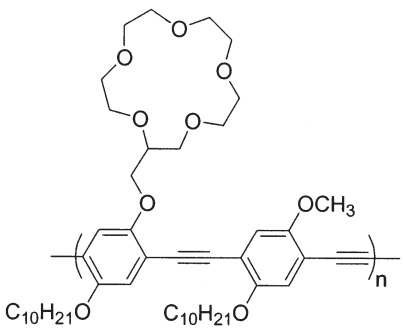

32

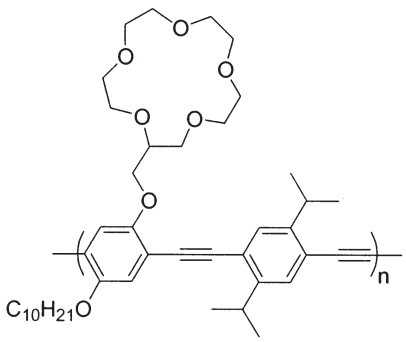

33

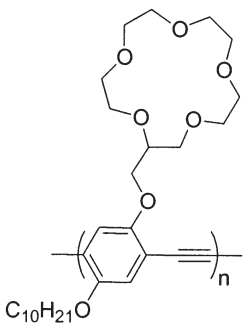

34

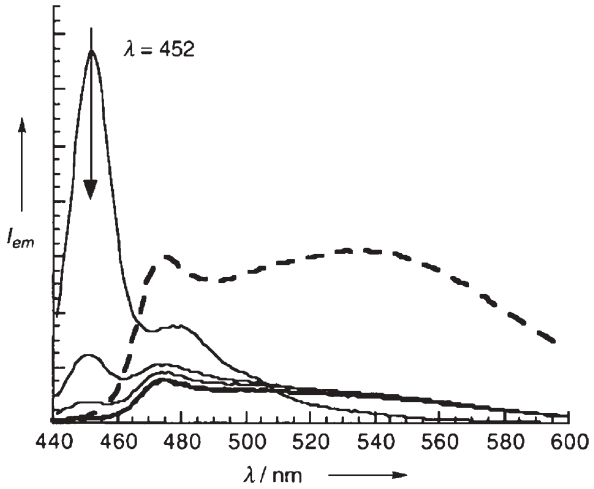

Fig. 8 Fluorescence spectra of polymer **29** with various mole ratios of K^+ ions. The *arrow* indicates the changes that result from increasing the concentration ratio of K^+ to 15-crown-5: 15-crown-5:K^+=1:0, 1:0.5, 1:1, 1:2.5, 1:5. *Dashed line* is data from a monolayer Langmuir–Blodgett film. (Reprinted with permission from Ref. [29]. Copyright 2000 Wiley-VCH Verlag GmbH)

mer chains. For instance, PPE **32** showed diminished aggregation efficiency due to competition from possible Lariat-type complexation between the crown ether and the adjacent methoxy oxygen. In **33**, the isopropyl side chains on the comonomer prevented π-stacking due to increased steric bulk. PPE **34** with crown ether moieties on every repeat unit could form intrachain complexes with K^+, so ion-induced interchain aggregation was absent.

In addition to metal ions, detection of halides such as fluoride is important, as the latter is often present in nerve gases and nuclear weapons manufacture. Our group utilized the unique reactivities of F^- with Si to specifically sense for fluoride ions [30]. PArE **35** was constructed with a masked precursor to a flu-

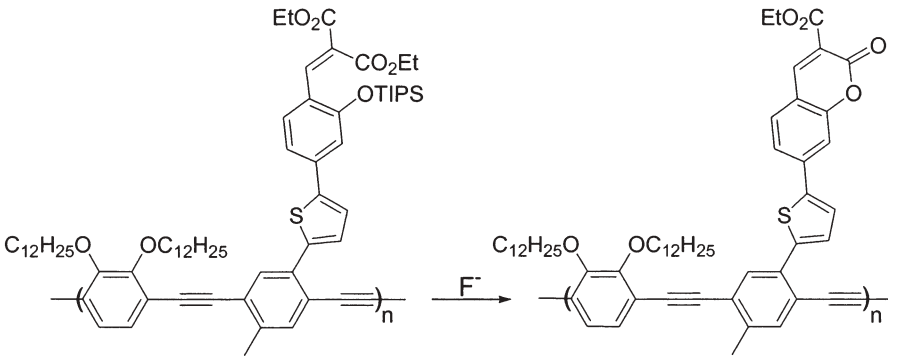

35 **36**

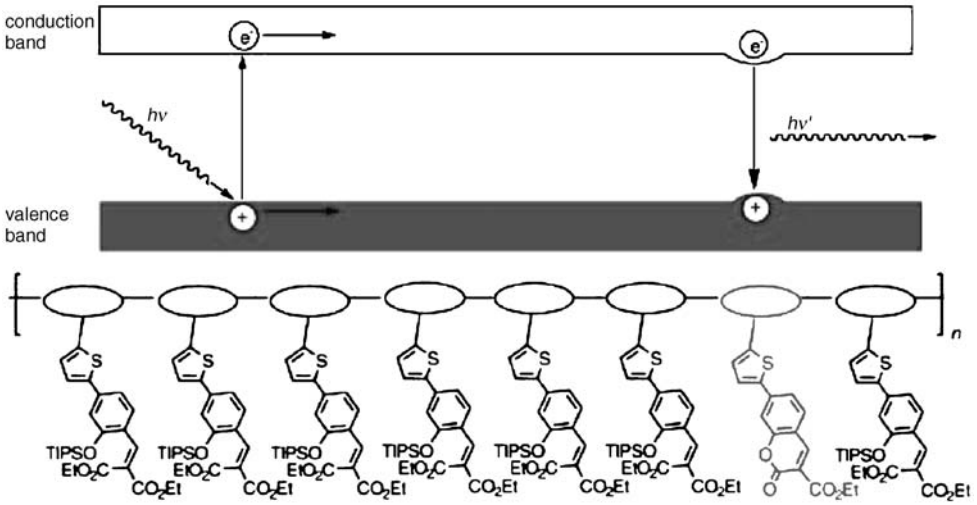

Fig. 9 Schematic band diagram depicting the mechanism by which a semiconductive polymer can produce an enhancement in PArE **34**. (Reprinted with permission from Ref. [30]. Copyright 2003 Wiley-VCH Verlag GmbH)

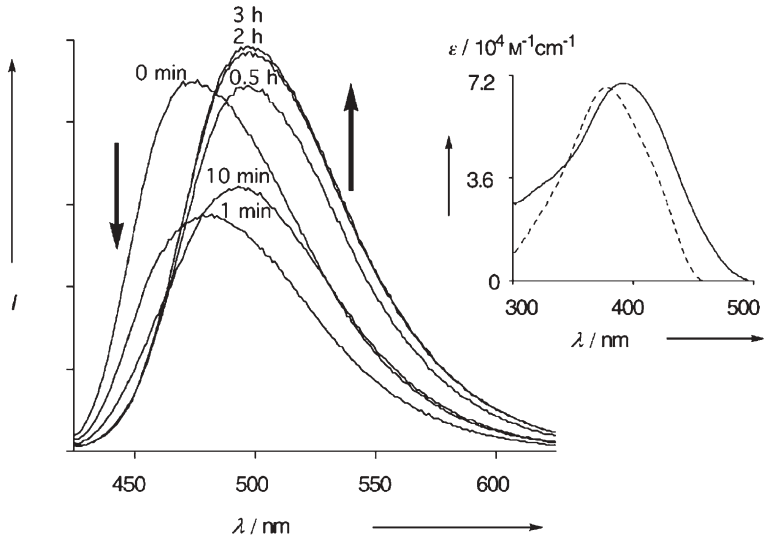

Fig. 10 Emission changes of polymer **33** upon addition of tetrabutylammonium fluoride (TBAF). *Inset* are the respective absorption spectra of the initial solution (0 min, ---) and after exposure to TBAF (—). 1.5×10^{-6} M in CH_2Cl_2 (repeating group) and TBAF, 1.6×10^{-7} M. (Reprinted with permission from Ref. [30]. Copyright 2003 Wiley-VCH Verlag GmbH)

orescent coumarin dye that is conjugated to the PArE. Upon exposure to fluoride ions, reaction with TIPS occurs and the coumarin dye forms to generate **36.** The electronic character of the dye is strongly coupled to the band structure of the PArE and locally perturbs the bandgap (Fig. 9). As a result, energy transfer occurs via the Dexter mechanism to the dye (Fig. 10). Under identical experimental conditions, the polymer proved to be 100-fold more sensitive to F^- compared to a simple masked coumarin, once again demonstrating amplification.

4 PArEs as Biosensors

The amplification ability of conjugated polymers can be used in biosensors and this capability becomes especially relevant considering the often minute quantities of biological analytes. Biological interactions such as those between proteins and their ligands, DNA strands, carbohydrates, and cells could all be potentially amplified using conjugated polymers. To be compatible with biological systems the polymer should be hydrophilic, and this is usually accomplished by installing ionic groups onto the polymer backbone. The transducer should also be highly selective, as it should only amplify the desired signal while minimizing the response due to nonspecific interactions.

As a proof of principle, the conjugated polymer MPS-PPV **6** with pendant sulfonate groups was used for sensing the interaction between biotin and avidin [11]. The strong association (K_a~10^{15} M) between the small molecule biotin and the tetrameric proteins avidin or streptavidin lends itself to a well-suited model system for biological recognition. As methyl viologen (MV^{2+}) is a good electron transfer quenching agent for conjugated polymers, a biotin-conjugated viologen was synthesized and added to a solution of MPS-PPV in water, resulting in a quenched polymer. Upon addition of avidin, the comparatively bulkier protein binds to biotin–viologen and removes it from the polymer, effecting an "unquench" (Fig. 11). Amounts of avidin on the order of 10^{-8} M can be detected. Limitations of this bioassay lie in the requirements for

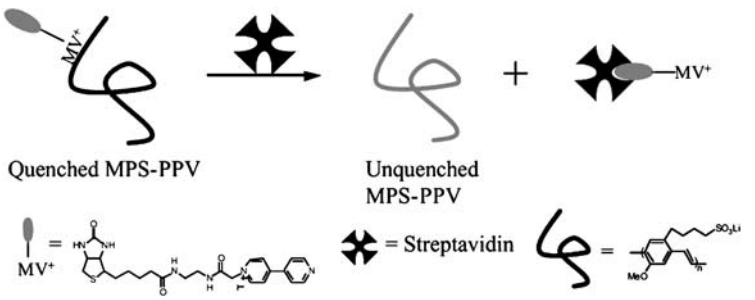

Fig. 11 Removal of a biotin-labeled quencher by avidin results in recovery of the MPS-PPV fluorescence.

the analyte. A protein that is too small may be unable to fully remove and segregate the quencher from the polymer. Changes in the charge of the quencher and in the protein may also affect the sensitivity of the ionic polymer.

Fluorescence recovery-type bioassays have also been designed by Heeger et al., utilizing a charge-neutral complex formed by the anionic sulfonated PPV **37**, MBL-PPV, and a cationic polyelectrolyte, poly(*N*,*N*-dimethylammonio-ethylene iodide) [31]. Both positively and negatively charged quenchers affect the photoluminescence of the polymer complex in phosphate-buffered saline (PBS), although at a decreased sensitivity corresponding to about 2 orders of magnitude compared to only the anionic PPV in water. The decreased sensitivity was attributed to a combination of ionic screening in the buffer solution and to the absence of static quenching for the neutral polymer complex. As a demonstration of the possible biosensing applications, a negatively charged dinitrophenol (DNP) derivative quenches the complex and this is reversed upon addition of anti-DNP IgG antibody.

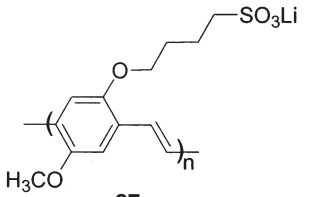

37

Electron transfer quenching analogous to that between MV^{2+} and PArEs is also possible with proteins. Fluorescence quenching of **37** was carried out with cytochrome c, a cationic protein, at neutral pH (pI=9.6 at room temperature) that can undergo rapid electron transfer [32]. An apparent K_{SV} for quenching of 3.2×10^8 M^{-1} at pH 7.4 was obtained and compared to the previously reported amplification factor of 67 [10]. However, the K_{SV} is a composite of the amplification factor and the binding constant of the protein to the polymer and so a fair comparison cannot be made. As can be expected in electrostatic complexations, the K_{SV} value was sensitive to the pH of the solution and dropped by up to 6 orders of magnitude when the pH was increased to >10 (where the protein was slightly anionic). Control experiments were conducted with myoglobin and lysozyme. No electron transfer could occur in the case of myoglobin; however, at a pH where it has the same surface charge as cytochrome c (at pH 7.4), a K_{SV} on the order of 10^6 M^{-1} could still be obtained. At pH 7.4, quenching of the polymer was also observed upon addition of the cationic lysozyme. There exists certainly some dependence of quenching efficiency on the electron transfer ability of the protein analyte. However, in this case the charge of the protein also plays a significant role in causing nonspecific quenching of the polymer, possibly by inducing aggregation and subsequent self-quenching.

Sulfonated **8** and biotinylated polymer **38**-coated streptavidin-derivatized polystyrene microspheres were useful as a platform for the detection of DNA

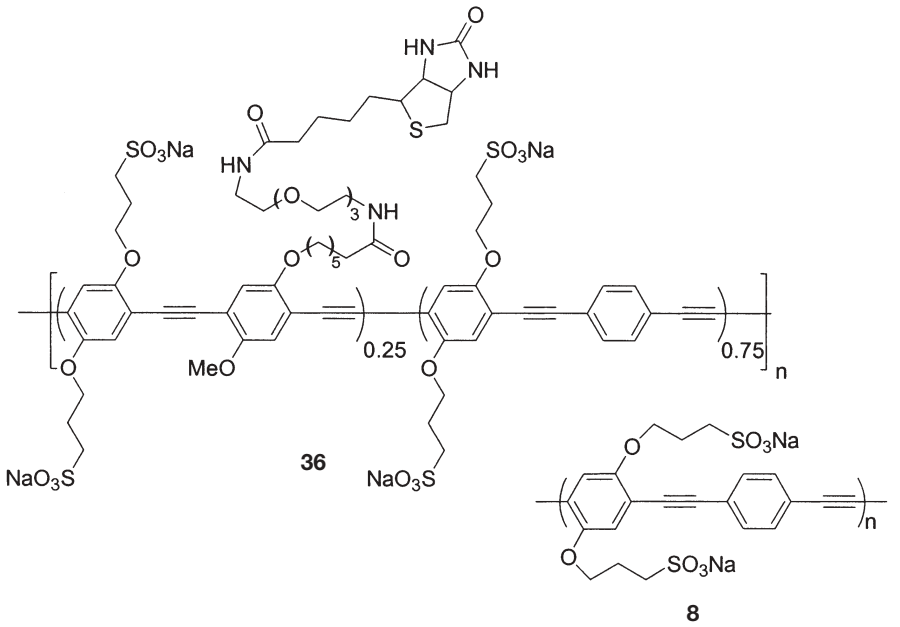

36

8

hybridization in competition assays [33]. A 20-base biotinylated capture DNA strand for anthrax lethal factor (ALF) was first bound to the microsphere. To this was added the quencher (QSY-7)-labeled complementary target strand. Quenching of the PPEs occurred upon hybridization of the target strand to the capture strand as the energy-accepting quencher was now brought into close proximity to the polymers (Fig. 12a). A series of competition assays were carried out. In the first case, the microspheres were subjected to a mixture of quencher-labeled target DNA and a nonlabeled ALF target strand. The QSY-7 DNA was kept constant while the concentration of the target strand was varied; it was expected that the quenching due to QSY-7 would be attenuated with increasing amounts of ALF target strand, as the latter would compete with the labeled DNA strand for the capture strand. However, little attenuation was observed even at higher concentrations of the target strand. The authors attribute this to a hydrophobic interaction between the quencher molecules with the polymers on the microsphere that enhanced preferential association of the

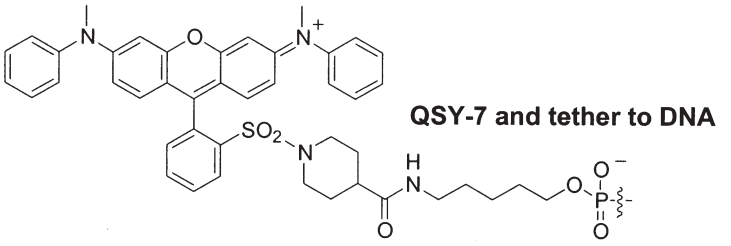

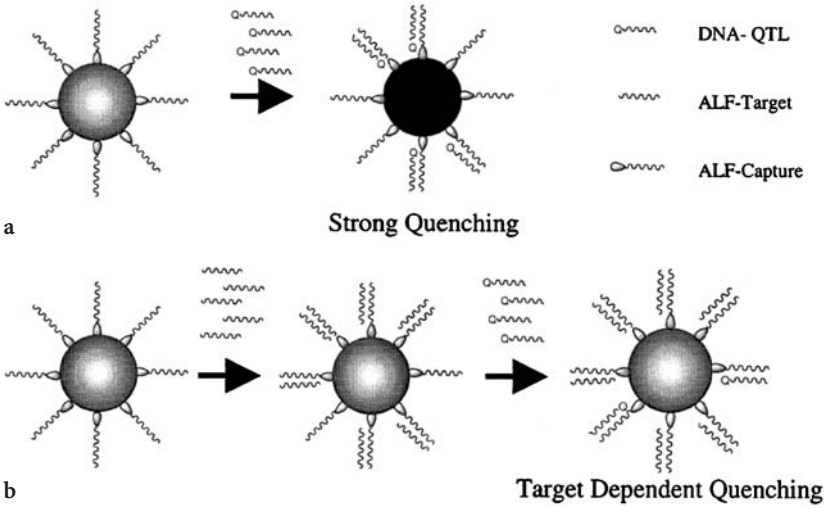

Fig. 12 **a** Quenching assay where QSY-7-labeled DNA strand (DNA-QTL) is presented to microsphere and microsphere-bound biotinylated ALF capture strand. **b** Competition assay for detection of target DNA. Variable amounts of ALF target are added to microsphere and bound ALF capture strand. This is then subjected to a fixed amount of QSY-7-labeled DNA. The amount of quenching is dependent on the amount of ALF target already bound on the microsphere. (Reprinted with permission from Ref. [33]. Copyright 2002 American Chemical Society)

QSY-7 conjugate. To circumvent this, variations on the competition assay were carried out. By a two-step sequential incubation of microsphere with varying amounts of ALF target strand followed by the QSY-7-labeled target DNA, attenuation of the level of quenching by the latter is observed (Fig. 12b). Alternatively the biotinylated capture strand, QSY-7 DNA, and variable amounts of ALF target could be incubated together. This mixture could then be added to the microspheres and similar attenuation of quenching was observed. By plotting the quenching ratio vs. the molar concentration of the ALF target, quenching attenuation curves were obtained. In a 200-µl assay containing 3.7×10^7 microspheres, 3 pmol of ALF capture strand, and 10 pmol of QSY-7-labeled complementary DNA, an attenuation of fluorescence can be observed at 0.5 pmol of ALF target. Thus, fluorescence recovery can be correlated to the amount of analyte oligonucleotide.

To elaborate upon this scheme, the authors replaced the DNA-based capture strand with one that is based on peptide nucleic acid (PNA) in order to distinguish single nucleotide mismatches [34]. Since PNA does not have a phosphodiester backbone, a PNA–DNA duplex is more thermodynamically stable than DNA–DNA or RNA–RNA helices due to a lack of electrostatic repulsion between the two chains. PNAs have also been shown to be more selective. However, PNAs are more difficult to synthesize and PNA–DNA interactions are not as well understood as DNA–DNA binding. In this study, quaternary ammo-

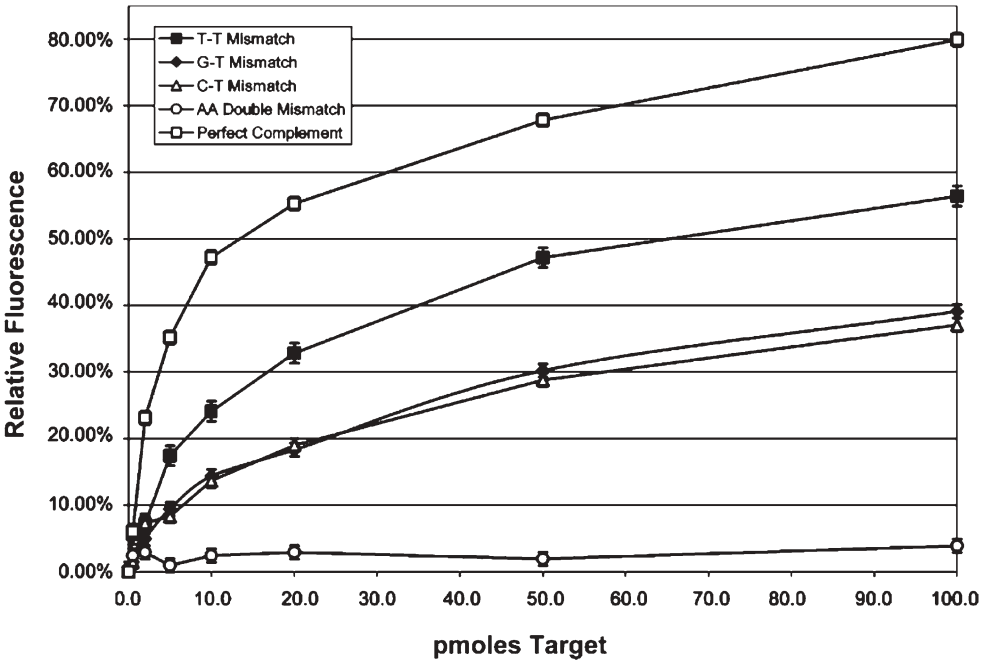

Fig. 13 Mismatch analysis at 40 °C using a microsphere sensor loaded with a PNA-based capture strand. T-T, G-T, C-T are single mismatch sequences. (Reprinted with permission from Ref. [34]. Copyright 2003 American Chemical Society)

nium-functionalized polystyrene beads were coated with a precomplexed solution of polymer **38** and neutravidin. By a similar competition assay to one previously described (Fig. 12b) using target sequences (mismatched or perfect complement) in variable amounts, a plot of the fluorescence ratio (before and after exposure to QSY-7-labeled target DNA) vs. the amount of ALF–DNA target sequence revealed the quenching attenuation as increasing amounts of the ALF–DNA competed for the hybridization sites. To improve the selectivity of the single mismatch in the 20-mer sequence, the assays were conducted at an elevated temperature of 40 °C, and mismatched sequences were expected to yield lower rates of quenching attenuation compared to that of the perfect complement. For a suspension containing 1×10^7 microspheres, 2 pmol bound PNA capture sequence, and 10 pmol QSY-7-labeled DNA target sequence, a 15% difference in quenching attenuation could be observed between the perfect complement and the mismatched sequences for 0.5 pmol of the various target ALF–DNA strands (Fig. 13). When the identical assay was performed at 25 °C with a DNA-based capture strand, poor resolution of the mismatched oligonucleotides was observed.

As a simple and practical alternative to coated microspheres, submicron particles of pendant amine-functionalized PPE **39** could be fabricated by phase

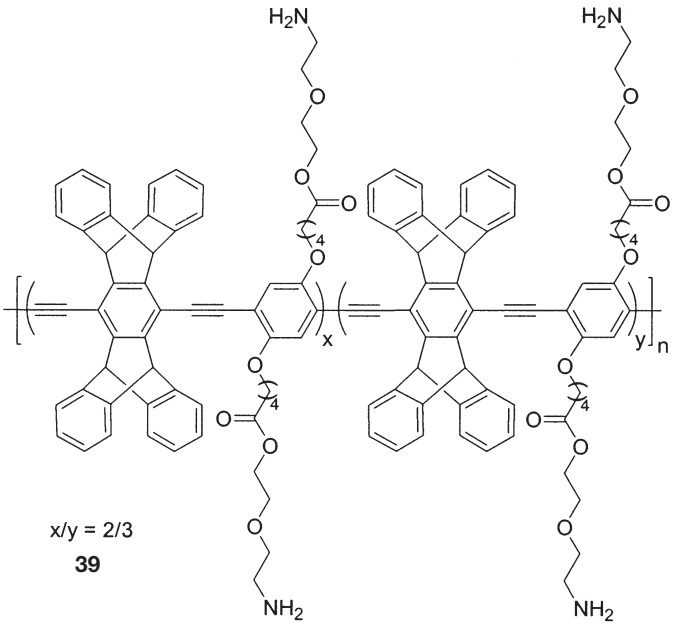

inversion and used for detecting Cy-5-labeled oligonucleotides [35]. While Cy-5 is well known as a fluorophore, the authors of this report use the dye as a quencher. Cy-5 concentrations in the range 10^{-10} to 10^{-7} M produced measurable quenching. A large K_{SV} of 8.8×10^{7} M^{-1} was obtained. The fluorescence quenching was 2 orders of magnitude more sensitive than direct excitation of the Cy-5 dye, and the platform could potentially be applied to DNA sensing arrays.

Carbohydrate detection is important for applications such as glucose monitors; these are arguably one of the most successful and relevant biosensors. An interesting fluorescence recovery-type saccharide sensor based on the reactivity of carbohydrates with boronic acids was reported in 2002 [36]. Specifically, modification of the cationic viologen-linked boronic acid derivative **40** to a zwitterionic species **41** upon covalent and reversible reaction of boronic acid with monosaccharides (Scheme 1) can cause the dissociation of the ion-pair in-

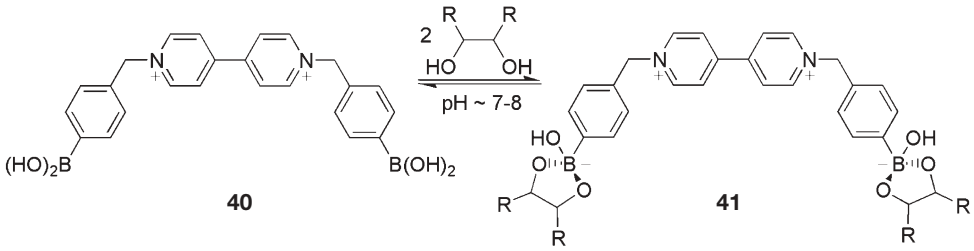

Scheme 1 Interaction between 4,4′-*N*,*N*′-bis(benzyl-4-boronic acid)-bipyridinium dibromide with a carbohydrate at near-neutral pH

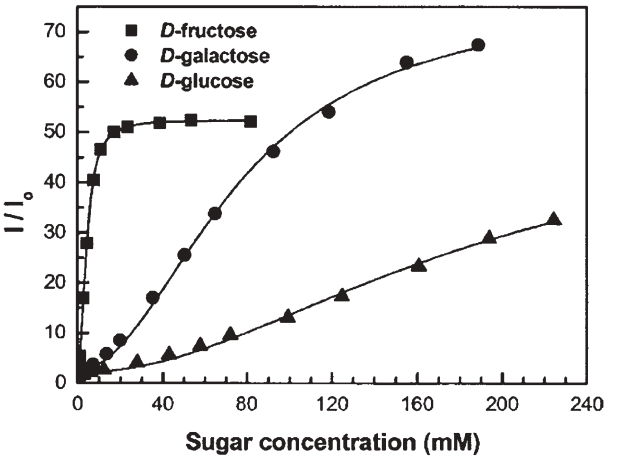

Fig. 14 Titration curves against sugar for PPE **8** (2.5×10^{-6} M)/**38** (8×10^{-7} M), measured in PBS (6 mM) of pH 7.4. (Reprinted with permission from Ref. [36]. Copyright 2002 American Chemical Society)

teraction between the viologen quencher and polymer **8**. This in turn leads to fluorescence recovery from the fluorescent polymer. In the case of galactose, up to 70-fold increase in fluorescence intensity was observed (Fig. 14).

PArE-induced aggregation of biological agents could potentially be used as a method of detection, considering the prevalence of multivalent interactions in biology. This was demonstrated by Bunz et al., who used a biotin-functionalized PPE and streptavidin-functionalized microspheres as a primitive model system for the recognition that occurs in cells and bacteria [37]. Upon incubation of the microspheres with PPE **42**, the solution fluorescence showed aggregation and the disappearance of a blue shoulder compared to the uncomplexed biotinylated polymer. Agglomeration of the microspheres was observed by scanning electron microscopy and fluorescence microscopy.

While quenching experiments are useful and provide a sensitive response to analytes, a turn-on sensor offers advantages such as improved sensitivity and selectivity to the species to be detected, as well as diminished response to non-

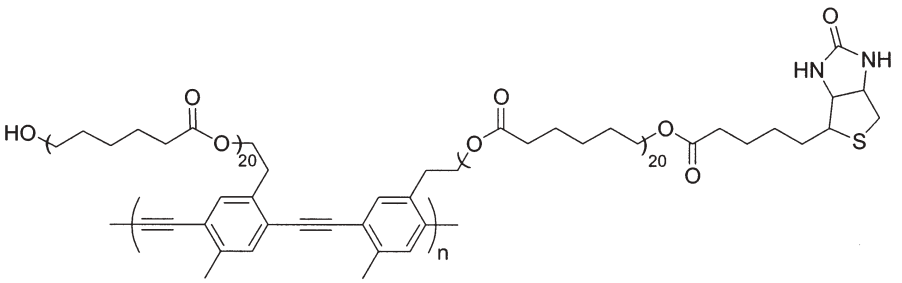

42

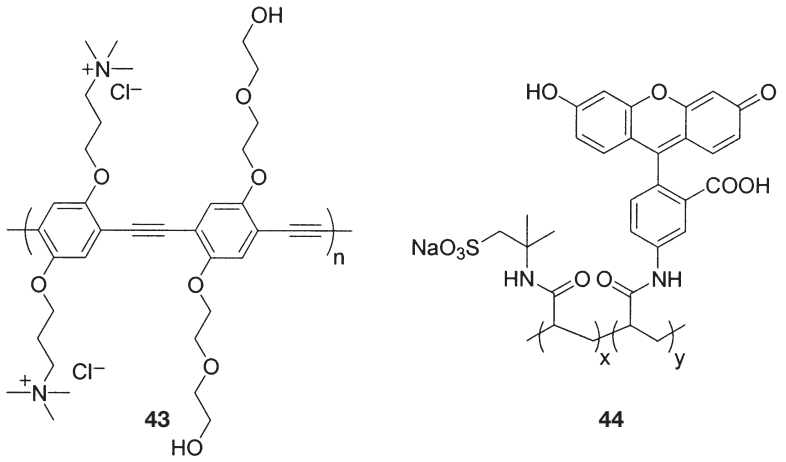

specific interactions. An obvious method is to use fluorescence resonance energy transfer (FRET) to transduce the recognition event. For this purpose our group demonstrated the efficient energy transfer from a PPE to a fluorescent pH-sensitive dye [38]. Films of cationic PPE **43** and the anionic fluoresceinamine-appended polyacrylate **44** were coated onto a glass substrate using layer-by-layer deposition. The absorption cross section, energy migration efficiency, and emission efficiency of the pendant fluoresceinamine dye could change as

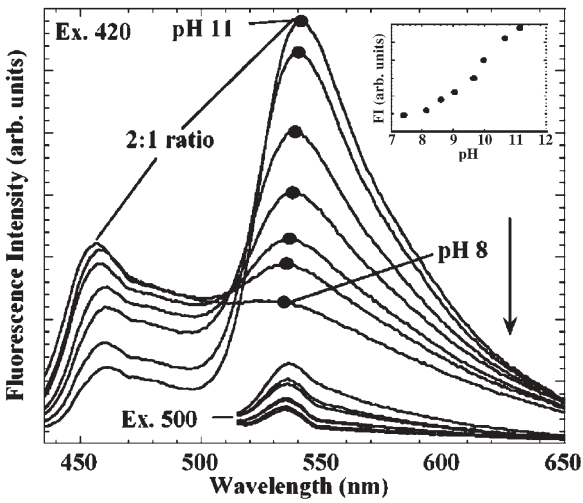

Fig. 15 A film composed of **42** sandwiched between two layers of **41**. The fluorescence spectra spanning 435 to 650 nm and the spectra beginning at 515 nm were excited at 420 and 500 nm, respectively. *Inset*: The emission maximum of the fluoresceinamine band after excitation at 420 nm plotted against pH. (Reprinted with permission from Ref. [38]. Copyright 2000 American Chemical Society)

a function of pH. At high pH, the dye is highly absorptive and fluorescent, acting as a shunt and withdrawing energy from the light-harvesting conjugated polymer. At low pH, the absorbance decreases and there is no fluorescence. Excitation of the PPE at 420 nm resulted in a tenfold increase in emission of the dye relative to its emission obtained by direct excitation. At pH 11, ~90% of the PPE's emission is transferred to the dye (Fig. 15). The architecture of the film is important; when **44** was sandwiched between two layers of **43**, more energy was transferred to the dye acceptor, as there was more energy-harvesting PPE available.

Based on these observations for FRET between PPE and fluorescent dyes, our group reported a model biosensor using biotinylated PPE **45** and dye-labeled streptavidin [39]. Upon binding of rhodamine B or Texas Red-X-labeled streptavidin to **45** in Tris buffer at pH 7.4, energy transfer to the dyes was observed. Surprisingly, Texas Red-X–streptavidin exhibited greater emission intensity, even though it has less spectral overlap (compared to rhodamine B–streptavidin) with the polymeric donor under identical experimental conditions (Fig. 16). This finding did not obey the requirements for Förster-type energy transfer, where diminished spectral overlap between the polymer donor's emission and the dye acceptor's absorption would result in decreased energy transfer. As Texas Red-X possesses a more planar structure and greater hydrophobic character compared to rhodamine B, once brought into close proximity to

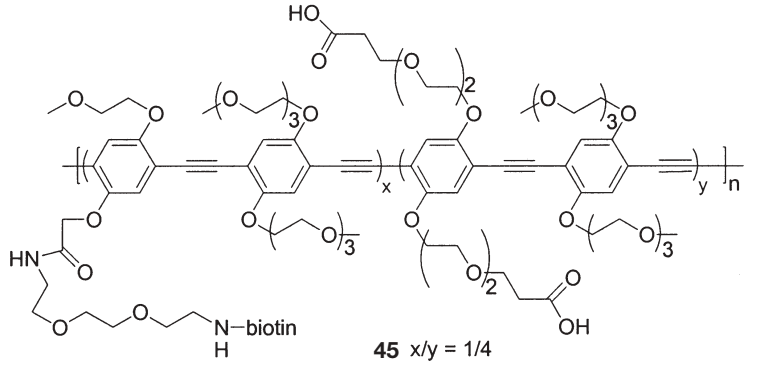

45 x/y = 1/4

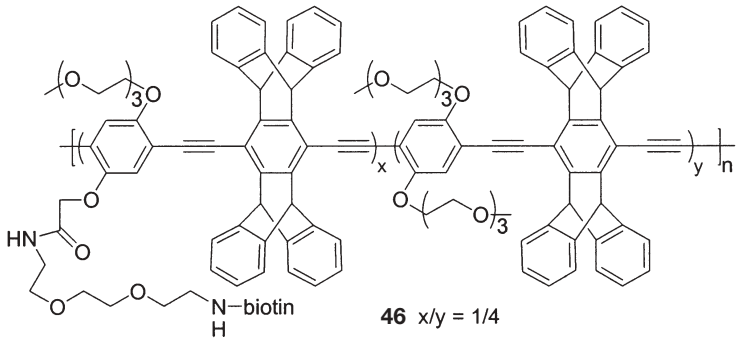

46 x/y = 1/4

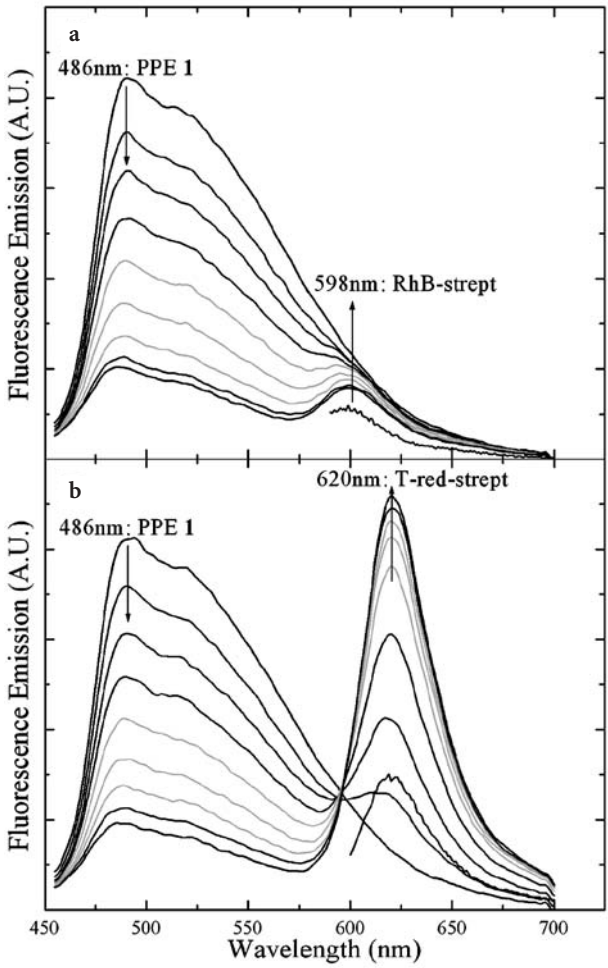

Fig. 16 Addition of 0.017-nmol aliquots of **a** rhodamine B-labeled streptavidin and **b** Texas Red-X-labeled streptavidin to 1.51 nmol of **43**. Energy transfer observed in both cases with amplified emission of the dyes to the light-harvesting conjugated polymers. Direct excitation of the dyes at 575 and 585 nm correspond to 0.100 nmol of streptavidin.

the polymer by the streptavidin–biotin recognition it may be able to interact more intimately with the polymer's phenylene ethynylene backbone and undergo greater orbital mixing. We proposed that a greater Dexter energy-transfer mechanism may be operative in this model system.

The interactions of the dye acceptors to polymers could also be witnessed in the case of solid films. In this case, the sterically more restrictive cavities of the polymeric film **46** allowed better orbital interaction with the smaller and more flexible rhodamine B dye, and accordingly higher energy transfer with rhodamine B-labeled streptavidin was observed compared to Texas Red-

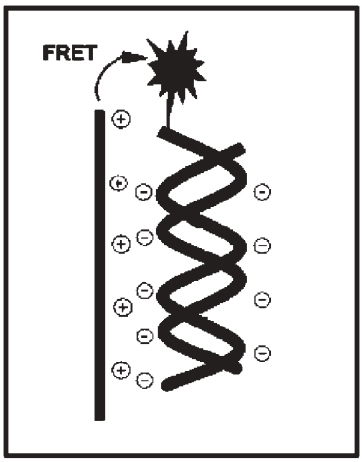

Fig. 17 Schematic representation of a DNA–DNA duplex bound electrostatically to polymer **45**. (Reprinted with permission from Ref. [44]. Copyright 2004 American Chemical Society)

X–streptavidin. The intricate interplay between the steric and electronic properties of the acceptor and the polymeric donor may have important impact for the design of future biosensors.

Some non-PArE based colorimetric and fluorometric sensors also deserve mention. Bazan et al. have used energy-transfer platforms in the design of sensors for detecting negatively charged PNA–DNA [40, 41], DNA–DNA [42–45] (Fig. 17), and RNA–peptide [46] duplexes. Typically these assays use cationic polymers such as **47**, a nonlabeled single-stranded capture DNA/RNA and a fluorophore-labeled complementary DNA/PNA/peptide. Upon formation of the recognition duplex, the fluorophore is brought into close proximity with the polymer by electrostatic interactions between the anionic duplex and cationic polymer; subsequent emission from the dye occurs due to energy transfer. A three-tiered energy-transfer assay has also been constructed [44] where energy transfer occurs from the conjugated polymer to a fluorescein-labeled DNA, which in turn transfers energy to an intercalated ethydium bromide. This could potentially improve selectivity and optical resolution of the biosensor.

Sensitive, cationic, water-soluble polythiophenes have been utilized for biosensing. Leclerc et al. have created affinitychromic sensors with such polymers for transducing a variety of recognition events such as those between

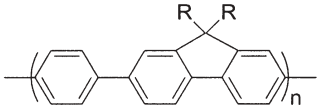

R = $(CH)_6\overset{+}{N}Me_3\,I^-$

47

biotinylated polythiophene–avidin, DNA–DNA, and aptamer–protein. Electrostatic and conformational differences that occur upon recognition disrupt the planarization and aggregation of the polymer backbone, leading to visible absorption and fluorescence changes. Remarkably, analyte detection levels down to 10^{-21} mol could in some cases be achieved [50]. Interested readers are referred to relevant publications [46–50].

Biosensors based on poly(diacetylene)s have also been investigated by other groups [51–54]. These have proved successful in detecting biologically relevant agents such as the influenza virus and cholera toxin.

5 Summary

Poly(arylene ethynylene)s have proven to be sensitive transducers capable of amplifying binding events ranging from detection of TNT and ions to detecting single mismatches in DNA. The ability to manipulate the properties of PArEs by changing their reactivities, assembly architecture, and emissive properties creates wide-ranging possibilities for practical real-life sensing purposes.

References

1. McQuade DT, Pullen AE, Swager TM (2000) Chem Rev 100:2537
2. Ofer D, Swager TM, Wrighton MS (1995) Chem Mater 7:418
3. Zotti G, Schiavon G, Zecchin S, Berlin A (1998) Synth Met 97:245
4. Greiner A (1998) Polym Adv Technol 9:371
5. Pschirer NG, Miteva T, Evans U, Roberts RS, Marshall AR, Neher D, Myrick ML, Bunz UHF (2001) Chem Mater 13:2691
6. Kocher C, Montali A, Smith P, Weder C (2001) Adv Funct Mater 11:31
7. Bunz UHF (2000) Chem Rev 100:1605
8. Swager TM, Gil CJ, Wrighton MS (1995) J Phys Chem 99:4886
9. Zhou Q, Swager TM (1995) J Am Chem Soc 117:7017
10. Zhou Q, Swager TM (1995) J Am Chem Soc 117:12593
11. Chen L, McBranch DW, Wang H-L, Helgeson R, Wudl F, Whitten DG (1999) Proc Natl Acad Sci U S A 96:12287
12. Tan C, Pinto MR, Schanze KS (2002) Chem Commun 446
13. Pinto MR, Kristal BM, Schanze KS (2003) Langmuir 19:6523
14. Jenekhe SA, Osaheni JA (1994) Science 265:765
15. Osaheni JA, Jenekhe SA (1995) J Am Chem Soc 117:7389
16. Kim J, Swager TM (2001) Nature 411:1030
17. (a) Levitus M, Schmieder K, Ricks H, Shimizu KD, Bunz UHF, Garcia-Garibay MA (2001) J Am Chem Soc 123:4259; (b) Levitus M, Schmieder K, Ricks H, Shimizu KD, Bunz UHF, Garcia-Garibay MA (2002) J Am Chem Soc 123:8181
18. Yang J-S, Swager TM (1998) J Am Chem Soc 120:5321
19. Yang J-S, Swager TM (1998) J Am Chem Soc 120:11864
20. Cumming JC, Aker C, Fisher M, Fox M, la Grone MJ, Reust D, Rockley MG, Swager TM, Towers E, Williams V (2001) IEEE Trans Geosci Remote Sens 39:1119

21. Levitsky IA, Kim J, Swager TM (1999) J Am Chem Soc 121:1466
22. Kim J, McQuade DT, Rose R, Zhu Z, Swager TM (2001) J Am Chem Soc 123:11488
23. Rose A, Lugmair CG, Swager TM (2001) J Am Chem Soc 123:11298
24. Wang B, Wasielewski MR (1997) J Am Chem Soc 119: 12
25. Liu B, Yu W-L, Pei J, Liu S-Y, Lai Y-H, Huang W (2001) Macromolecules 34:7932
26. Zhang Y, Murphy CB, Jones WE Jr (2002) Macromolecules 35:630
27. Jiang B, Yang S-W, Barbini DC, Jones WE Jr (1998) Chem Commun 213
28. Bangcuyo CG, Ranpey-Vaughn ME, Quan LT, Angel SM, Smith MD, Bunz UHF (2002) Macromolecules 35:1563
29. Kim J, McQuade DT, McHugh SK, Swager TM (2000) Angew Chem Int Ed 39:3868
30. Kim T-H, Swager TM (2003) Angew Chem Int Ed 42:4803
31. Wang D, Gong X, Heeger PS, Rininsland F, Bazan GC, Heeger AJ (2002) Proc Natl Acad Sci U S A 99:49
32. Fan C, Plaxco KW, Heeger AJ (2002) J Am Chem Soc 124:5642
33. Kushon SA, Ley KD, Bradford K, Jones RM, McBranch D, Whitten D (2002) Langmuir 18:7245
34. Kushon SA, Bradford K, Marin V, Suhrada C, Armitage BA, McBranch D, Whitten D (2003) Langmuir 19:6456
35. Moon JH, Deans R, Krueger E, Hancock LF (2003) Chem Commun 104
36. DiCesare N, Pinto MR, Schanze KS, Lakowicz JR (2002) Langmuir 18:7785
37. Wilson JN, Wang Y, Lavigne JJ, Bunz UHF (2003) Chem Commun 1626
38. McQuade DT, Hegedus AH, Swager TM (2000) J Am Chem Soc 122:12389
39. Zheng J, Swager TM (2004) Chem Commun 2798
40. Gaylord BS, Heeger AJ, Bazan GC (2002) Proc Natl Acad Sci U S A 99:10954
41. Liu B, Bazan GC (2004) J Am Chem Soc 126:1942
42. Gaylord BS, Heeger AJ, Bazan GC (2003) J Am Chem Soc 125:896
43. Liu B, Gaylord BS, Wang S, Bazan GC (2003) J Am Chem Soc 125:6705
44. Wang S, Gaylord BS, Bazan GC (2004) J Am Chem Soc 126:5446
45. Wang S, Bazan GC (2003) Adv Mater 15:1425
46. Leclerc M, Ho H-A (2004) Synlett 2:380
47. Leclerc M (1999) Adv Mater 11:1491
48. Bernier S, Garreau S, Béra-Abérem M, Gravel C, Leclerc M (2002) J Am Chem Soc 124:12463
49. Ho H-A, Leclerc M (2004) J Am Chem Soc 126:1384
50. Doré K, Dubus S, Ho H-A, Lévesque I, Brunette M, Corbeil G, Boissinot M, Boivin G, Bergeron MG, Boudreau D, Leclerc M (2004) J Am Chem Soc 126:4240
51. Charych DH, Nagy JO, Spevak W, Bednarski MD (1993) Science 261:585
52. Reichert A, Nagy JO, Spevak W, Charych D (1995) J Am Chem Soc 117:829
53. Pan JJ, Charych D (1997) Langmuir 13:1365
54. Song J, Cheng Q, Zhu S, Stevens RC (2002) Biomed Microdevices 4:213